

**AN INVESTIGATION OF A TAILLESS AIRPLANE**

**A THESIS**

**Submitted in partial fulfillment  
of the requirements for the Degree  
of Master of Science in Aeronautical Engineering**

**by**

**Charles B. Rumsey**

**Georgia School of Technology  
Atlanta, Georgia  
1943**

013 9-1-43

69237

11

AN INVESTIGATION OF A TAILLESS AIRPLANE

Approved:

Date Approved by Chairman 5/15/43

## ACKNOWLEDGMENTS

The author wishes to thank Professor Montgomery Knight and Professor Alan Pope for their many helpful suggestions during this investigation, and Mr. W. C. Slocum for his suggestions on the construction of the wind tunnel model.

## TABLE OF CONTENTS

	Page
Approval Sheet .....	ii
Acknowledgments .....	iii
Summary .....	1
Introduction .....	2
Models and apparatus .....	4
Procedure .....	8
Discussion .....	26
Conclusions .....	32
BIBLIOGRAPHY .....	33
APPENDIX .....	34
TABLES	
FIGURES	

## AN INVESTIGATION OF A TAILLESS AIRPLANE

### SUMMARY

An investigation was made to determine the aerodynamic characteristics and longitudinal stability of a flying wing airplane of the type shown in Figure 1. The most important characteristic of the design is the bending down of the tips along non-parallel lines, which gives them a negative angle of incidence relative to the panel of the wing.

The results indicate that the airplane will possess dynamic longitudinal stability at all speeds above, and probably at, that of stalling, and that the maximum value of the lift over drag ratio of the design is approximately the same as that of clean, conventional airplanes.

Although the design exhibited no unusual aerodynamic characteristics, with the exception of good longitudinal stability near the stall, the general physical outline would be advantageous in a military airplane where an unrestricted field of gunfire is desirable. It might also prove to be an economical commercial type, being much less complex in structure than the conventional airplane, and having a large amount of available space within the thick wing.

Further investigation of this type of flying wing, especially in regard to lateral stability and control, seems desirable.

## INTRODUCTION

Shortly after the present investigation was begun, some pictures and a very limited amount of information were published concerning the Northrop Flying Wing. The pictures showed the planform to be very similar to that herein used. Although the tips were bent down, it is not believed that negative tip incidence due to non-parallel bend lines was used. Good stability and control and exceptional performance are claimed for the airplane, but, since all such information has been kept confidential, no comparison can be made between it and the tested design.

Several other flying wing airplanes have been built and flown, some with a certain measure of success. The best known of these were the Westland-Hill "Pterodactyl" series, built about 1934, and the Dunn tailless biplane, flown somewhat earlier.

The Dunn machine had wings of constant chord and approximately thirty degrees sweepback. Washout at the wing tips gave a stabilizing down load acting considerably behind the center of gravity due to the large amount of sweepback. This airplane was reported to be extremely stable.

The "Pterodactyl" type (Reference 6) was a monoplane with short, nacelle-like fuselage. The wing was of tapered planform with swept back leading and trailing edges. Flaps on the trailing edges acted together as elevators and differentially as ailerons. The sweepback was such that these flaps were approximately one chord length behind the trailing edge of the center section. One of the "Pterodactyl" airplanes used an arrangement whereby the sweepback of the wing could be varied in flight,

thus trimming the airplane for varying load and speed conditions.

The "Pterodactyl" series was considered to be slightly better than neutrally stable and of reasonable controllability. Its worst feature was a tendency to develop a phugoid oscillation at take-off if "pulled off" rather than "flown off" the ground.

This phugoid oscillation, though not always causing take-off difficulties, appears to be one of the most difficult problems to overcome in the design of a satisfactory tailless airplane.

The purpose of this investigation was to determine the characteristics of the phugoid oscillation of a flying wing airplane having bent down tips with negative incidence, and to determine the aerodynamic characteristics of the design by means of wind tunnel force tests.

## MODELS AND APPARATUS

The model constructed for the wind tunnel tests is shown in Figures 1 and 2. It was cut from a laminated mahogany block. The panel is made in one piece and then cut and rejoined to form the dihedral angle. The tips were made separately and then fastened to the panel by means of simple hinges which were rigid when tightened, but allowed the angle of depression of the tips to be adjusted. The space between the tip and panel was filled and faired with modeling clay.

All tests were made in the small wind tunnel of the Daniel Guggenheim School of Aeronautics at The Georgia School of Technology. The working section of the tunnel is two and one-half feet square, and, for these tests, was used with an open throat. A complete description of the tunnel and balance system is given in Reference 4. The wire support system therein described, and visible in Figure 3, was also used for the static tests made on the flying wing model.

An analysis of the dynamic longitudinal stability required that a measurement of the damping in pitch be made. For this purpose an oscillating model support, similar to that used in Reference 2, was constructed. Figure 4 is a sketch of the oscillator, while Figures 5 and 6 are photographs showing the model mounted on the oscillator and the apparatus set up in the wind tunnel. The oscillating parts are suspended on an axis and held in the wind tunnel by the springs, with the model at the angle of attack under consideration. The springs produce a restoring moment so that any slight rotation of the model in pitch tends to be corrected. If the model be then slightly displaced it will oscillate



about the axis under the action of the restoring moment, due to the springs, and under the action of the wind forces upon the model. As the experiments were to be conducted at four different angles of attack it was necessary to have the springs adjustable so that the model could be held at the correct initial attitude in the wind stream. Hook's Law was assumed, so that regardless of the initial tension in the springs, the restoring moment for a given slight displacement was always the same.

To keep the mechanical friction at a minimum was the biggest problem in the construction of the oscillator. For this reason, needle points, resting in conical depressions, were used for the main support bearings and also for the spring clips where they were attached to the transverse arm. The main support needle points were made of hardened steel and carefully ground and lapped to an extremely small, but smooth, spherical radius. The conical depressions in which the points rested were first drilled and then lapped in hardened steel inserts which were then driven into holes drilled for this purpose in the main shaft of the oscillator. In the case of the clips which held the springs on the transverse arm, the whole clip, part of which formed the needle point, was hardened. The two portions of the transverse arm which contained the depressions for the clip needle points were hardened after the depressions had been drilled.

The position of the weights on the transverse arm could be varied in order to change the period of oscillation of the apparatus, which, for the tests, was approximately one half second.

Each of the two sets of springs which insured oscillatory motion

had a constant of 9.8 pounds per inch. This gave them sufficient strength to hold the apparatus on the bearing points against the wind forces, and to impart enough energy to the system due to the initial displacement to make the oscillation persist for a reasonable time. With the bearing friction minimized by hardening and finishing the points and seats, the apparatus with model in place oscillated in still air for more than three minutes before the motion subsided to one ninth of the initial displacement of three degrees. This motion was considered persistent enough to allow an accurate measurement to be made of the time required for the oscillation to be damped by the wind tunnel air stream.

An accurate measurement of the time required to damp the oscillation necessitated that there be some means of magnifying the motion. This was accomplished by mounting a mirror on the end of the main shaft of the oscillator, the mirror being in a vertical plane but at forty-five degrees to the axis of the shaft. An opaque projector slide was prepared, having only a very small pin point aperture through which the light could pass. A hair was stretched across the center of the aperture to give a reference line. When the projector, with the slide in place, was directed at the mirror from a location on the extended axis of the shaft, the light was reflected ninety degrees and could be focused on a board at the far end of the laboratory. The shadow of the hair gave a quite sharp reference line, and the distance from mirror to board was such as to give a deflection of more than two feet for a three degree rotation of the shaft.

To measure the angular deflection of the shaft, and thus the

angle of attack of the model supported on the shaft extension, a flat surface was machined on the top side of the shaft. The angle of the machined surface to the horizontal was measured by means of an inclinometer. Knowing the angle between the chord line of the model and the machined surface, the angle of attack of the model was easily determined. Figure 5 shows the inclinometer in place to measure the angle of attack.

One other important point regarding the oscillating apparatus was that if the damping coefficient determined from the tests was to be proportional to that of the full-size airplane, the model must oscillate about the point where the center of gravity of the full-size airplane would be located. Adjustment of the model position with respect to the main shaft of the oscillator was provided for by attaching the model support arm to the main shaft with set screws. Figures 5 and 6 show this adjustable attachment.

## PROCEDURE

To determine the fundamental proportions of a flying wing of this type which would have reasonably good flying characteristics, many small cardboard and solid balsa wood models were made and glide-tested. These models did not prove to be very satisfactory since a very high wing loading resulted from building them with a reasonably stiff wing. All of these preliminary models showed a more or less pronounced "phugoid", or relatively long period, lightly damped longitudinal oscillation. From them, however, tentative values of sweepback, angle of tip bend line with thrust line, and the ratio of tip area to panel area were decided on.

This type of flying wing is not purely an airfoil since the wing tips, being bent down along non-parallel, forward converging bend lines, operate normally at small negative angles of attack, and, being behind the center of gravity due to the sweepback, act as balancing surfaces, or stabilizers. The moment arm of this stabilizing down "tail load" is, however, so short that it was believed that an airfoil section with as much inherent stability and as little center of pressure travel as possible would give the best results. As first choice, the M-24, an airfoil shape with reflex camber and small center of pressure travel, was decided on. Using this section, a spar and rib construction model was built of balsa wood and covered with doped tissue. The wing span was two and one-third feet and the general plan form was very similar to that of the final wind tunnel model.

This model proved itself in glide tests to be, at best, neutrally stable and that only for one very definite center of gravity location.

Any slight change from this center of gravity location caused it to become very unstable. Even with the correct center of gravity location, practically all of the glides ended by the model very suddenly going into a nose dive, which, if the height was great enough, continued past the vertical until the model was on its back.

It was attempted to improve the stability of the model by mounting the wing tips upside down. Since the tips operated at negative angles of attack they should be more effective if their camber were in the inverse sense. Increasing the "tail load" in this way, however, did not noticeably improve the stability.

From a consideration of the performance of this first model, it was decided to try a symmetrical airfoil section and thus be rid of the moment about the quarter-chord point which is common to cambered airfoils. This change was made since it seemed reasonable to assume that the best center of gravity location would be slightly ahead of the quarter-chord point of the mean aerodynamic chord.

The second glider built was of the same general proportions as the first, but using the symmetrical 0021 airfoil section. This section is 21 per cent of the chord length in thickness, and was used because in the full-size airplane it would give enough room for the internal housing of the engines, besides allowing space for all other required items, except possibly for a portion of the cockpit.

The center of gravity of this model was made accurately adjustable by cementing a small wooden screw to the upper surface on the center line, and running two steel nuts backwards or forwards on it as desired.

The angle of depression of the wing tips relative to the panel

was made adjustable on this model, as it was on the first. This was done by fastening the tips to the panel with short pieces of soft iron wire. The wire was rigid enough to hold the tips in place, but could be easily bent to adjust the angle of depression.

Figure 7 is a photograph of this glider.

This model gave fairly satisfactory glides; especially when catapulted from a simple rubber sling. The angle of glide was much better when the model was launched in this manner than when launched by hand. Also, many glides were made during which no phugoid oscillation was noticed.

The center of gravity location was quite critical for this model, although not nearly so critical as for the first model. Stability could be retained for small shifts of the center of gravity by changing the depression of the tips. Differential tip adjustment resulted in steady banked turns when the glider was launched by catapult, and a slight depression of both tips below the position for best glide made the glider climb as it left the catapult, although the glide after the climb was not as stable as that with the tips set for a normal glide.

The quarter-chord point of the mean aerodynamic chord of the panel was marked on the glider. By balancing the glider on a knife edge, the longitudinal center of gravity could be found. It was evident from a number of trials, that the location of the center of gravity which gave the best glides was a point very near the quarter-chord point of the mean aerodynamic chord, preferably, slightly ahead.

Changes were made in this model in the hope of improving the glide ratio and the stability, neither of which was as good as is usual with

conventional type airplane models. The first change made was to use cambered wing tips, the camber being in the negative sense to increase the down load. With these tips, the stability was less than it had been with the symmetrical tips.

The second change was to increase the tip area. Symmetrical section tips of approximately 75 per cent greater area were tried. The stability seemed slightly improved, but the angle of glide was steeper.

It was decided to proceed with the investigation on the basis of the original symmetrical model, which was the most promising. The wind tunnel model was built using the proportions of this glider, with the exception of the tip area which was increased from 17 per cent to 22.6 per cent of the total wing area. The dimensions of the wind tunnel model are given in Figure 1.

Static tests for lift, drag, and pitching moment were made with the model supported in the wind tunnel by the usual balance system. Tests for these characteristics were made with the model in each of the following conditions: 1. tips removed, 2. tips at zero angle with the panel, 3. depressed 10 degrees, 4. depressed 25 degrees, and 5. depressed 40 degrees. The tip depression angle was measured along the trailing edges of the tip and panel by means of a machinist's protractor, care being taken that the angle measured was normal to the chord line. During each of the five runs the angle of attack was varied by approximately three degree intervals, from an angle of attack that gave a definite negative lift to at least three degrees beyond the stall. From the data taken, curves of  $C_L$ ,  $C_D$  and  $C_m$  were plotted versus angle of attack. A polar plot of  $C_L$  versus  $C_D$  and a curve showing the variation of lift over drag ratio with angle of attack were also made. These curves are shown

in Figures 8 through 12. All coefficients were based on the area of the panel only. The coefficients of lift and drag were corrected for wind tunnel wall interference as suggested in Reference 7. The moment coefficient was calculated to be that about the quarter-chord point of the mean aerodynamic chord of the panel.

The oscillator described previously was used for the determination of the damping of the model in pitch, which was needed, in addition to the static characteristics, for the analysis of longitudinal stability.

With the model mounted on the oscillator the apparatus was adjusted so that the quarter-chord point of the mean aerodynamic chord of the panel was on the axis of rotation. The apparatus was then set up at the mouth of the tunnel as shown in Figure 6. This photograph was taken inside the tunnel, up-stream from the model. It can be seen that with the model in the center of the wind stream, the oscillator was only slightly outside of the direct airstream. Had the model been moved farther out on the support arm, however, there would have been possibilities that the support arm would bend or vibrate due to the air loads on the model, and cause the model to move with respect to the axis of rotation.

With the model in position, the tunnel speed was adjusted to a velocity corresponding to a  $q$  of  $25 \text{ K/M}^2$ . The beam of light from the projector was then directed at the mirror on the oscillator shaft and focused on the board as previously described. By means of adjustable blocks placed under the transverse arm of the oscillator, the angle of attack of the model, as measured by the inclinometer, was adjusted to the value desired for the initial attitude about which the oscillation



was to take place. With the apparatus held in this attitude, the position of the reflected hair line was marked on the board. The model was then deflected three degrees in pitch from this initial attitude and held while the new position of the hairline was marked. The procedure was again repeated to mark the position of the hair line when the amplitude of the deflection was one quarter of the initial three degrees displacement.

All restraint was then removed from the oscillator, and with the tunnel speed still that for a  $q$  of  $25 \text{ K/M}^2$ , the springs were adjusted until the hair line was at the position on the board indicating the angle of attack of the initial attitude. With the apparatus unrestrained and the model in the wind stream, some very slight oscillation was unavoidable. It was so small, however, that the hair line on the board moved up and down a distance only slightly greater than its own width, and an accurate adjustment could be easily made.

To measure the damping due to the wind forces on the model and apparatus, the system was deflected through an initial displacement of three degrees, as indicated by the marked position for the hair line. The time, from the instant of release to the instant when the oscillation had been damped to one quarter, as indicated by the hair line's coming to rest on the correspondingly marked position at the maximum amplitude of an oscillation, was measured by means of a stop watch. This time was an indication of the damping of the model and apparatus. To find the damping due to the model alone, the same procedure as described for the model and apparatus was repeated for the apparatus with the model removed. The measured time was then due to mechanical and wind damping

of the apparatus. The difference between the two subsequently calculated coefficients for model and apparatus, and apparatus alone, indicated the damping of the wind forces on the model alone.

Measurements of the time to damp to one quarter were made with the model oscillating about four different initial angles of attack; namely, two and one-half degrees, five degrees, eight degrees and eleven degrees, representing a range of airspeeds from high speed to near stalling for the full-size airplane.

It also should be stated that the entire investigation of longitudinal dynamic stability was carried out with a tip depression angle of twenty-five degrees, since that adjustment of the model afforded the best range of static stability as shown by the static pitching moment coefficient curves.

As stated, the difference between the damping coefficient calculated from the time to damp model and apparatus to one quarter and that calculated from the time to damp the apparatus alone to one quarter is the measure of the damping of the model alone. For each case, model and apparatus, and apparatus alone, the indication of damping is the time required to damp to one quarter.

In order to transform this indication of damping into the actual damping coefficient in pitch, the general transient solution of an oscillatory system of one degree of freedom must be considered. From Reference 3, this may be written in the form

$$X = D e^{-\frac{C}{2I} t} \sin(\omega_n t + \psi)$$

where

$X$  = amplitude at time  $t$

$D$  = constant of integration

$c$  = damping coefficient

$I$  = moment of inertia of all oscillating parts

$\omega_n$  = the natural angular frequency

$\psi$  = the phase angle

Then, if measurement of the amplitude  $X$  is made only at points of maximum amplitude, and two such maximum amplitudes are designated  $X_1$  and  $X_2$ ,

$$\frac{X_1}{X_2} = \frac{De^{-\frac{c}{2I}t_1} \sin(\omega_n t_1 + \psi)}{De^{-\frac{c}{2I}t_2} \sin(\omega_n t_2 + \psi)}$$

Now if  $X_1$  is the initial amplitude, and the time is measured from the instant of release so that  $t_1 = 0$ , then

$$\frac{X_1}{X_2} = e^{\frac{c}{2I}t}$$

or

$$\log \left( \frac{X_1}{X_2} \right) = \frac{c}{2I} t$$

In the tests made,  $X_2$  was one quarter of  $X_1$ , the initial displacement, so for the determination of the damping coefficient  $C$ ,

$$\log 4 = \frac{c}{2I} t$$

where  $t$  is the time in seconds required to damp to one quarter.

Before calculating the model damping coefficient, the moment of inertia of all oscillating parts was needed.

The moment of inertia about the center of rotation of all moving parts of the oscillator was calculated with the exception of the springs,

it being assumed that the effect of their motion was negligible.

The method described in Reference 5 was used to determine the moment of inertia of the model. This method required that the model be swung in a cradle, and the period of oscillation be timed. A cradle, consisting of two triangular frames of very light balsa wood, was constructed. The frames were hung from a quarter inch diameter steel rod, with two small pieces of razor blade glued to the frames acting as bearing edges. A sketch of the cradle is shown in Figure 13.

The model was placed in the cradle, the distance from the center of gravity of the model to the bearing edges measured, and the period of a very small swinging oscillation measured. From these measurements the moment of inertia of the model was calculated. The construction of the cradle was so light that its effects on the location of the center of gravity were considered negligible.

Also, the center of gravity of the model was extremely close to the quarter-chord point of the mean aerodynamic chord of the panel, so that the moment of inertia about the lateral axis through the center of gravity was considered to be the moment of inertia about the Y-Y axis, which passes through the quarter-chord point.

Measurements were made with the model supported in the cradle in two different positions, and the average of the two resultant moments of inertia, which were in close agreement, was added to the calculated moment of inertia of the moving parts of the apparatus. This value, the moment of inertia of all oscillating parts with the exception of the springs, was used along with the time,  $t$ , to calculate the damping coefficient of the model in pitch from the equation on Page 15.

Results of the oscillation tests are given in Table I.

At this point in the investigation it was necessary to consider the full-size airplane. The following physical characteristics were estimated and assumed for a full-size flying wing, geometrically similar to the previously tested wind tunnel model.

$$\frac{W}{S} = 15.45 \text{ lbs./ft.}^2$$

$$S_p = 191.9 \text{ ft.}^2 \text{ (Panel area) Total area} = 222 \text{ ft.}^2$$

$$b = 40 \text{ ft.}$$

$$W = 2660 \text{ lbs.}$$

#### Weights:

Structural weight	-	1520 lbs.
Engines ( 2 at 125 HP )	-	500 lbs.
Landing gear (3 wheels)	-	150 lbs.
Gas and oil (approx. 35 gals.)	-	240 lbs.
Pilot and equipment	-	<u>250</u> lbs.
Total	-	2660 lbs.

Power loading	-	11.02 lbs/HP
Endurance	-	approximately 3 hours
Top speed	-	approximately 193 m.p.h.
Stalling speed no flaps	-	approximately 80 m.p.h.

To calculate the moment of inertia of the full-size airplane, the wing structure was considered separately, and later added to the smaller moments of inertia due to the other items. To simplify the calculation for the structure, the wing was considered to have the correct plan form, but a rectangular cross section, and a mass distribution proportional to the volume. The moment of inertia about the lateral axis through the center of gravity of this "box wing" was found, and assumed to be the moment of inertia of the true airfoil section wing about the quarter panel mean aerodynamic chord point. The positions of the remaining items were then estimated and their moments of inertia about the lateral axis through the quarter panel mean aerodynamic chord point calculated. The sum of the moments of inertia of all the parts gave what was believed to be a reasonable value of  $I_{yy}$  for a flying wing airplane of this size and design.

From the tests and calculations described, all of the characteristics of the airplane needed for an analytical investigation of dynamic longitudinal stability of the full-size flying wing are known.

The system of axes used in the analysis is shown in Figure 14 along with a table of symbols for the motions with respect to these axes. The axes are such that the X axis will lie in the direction of the relative wind,  $U$ , for the initial undisturbed motion, the Y axis will extend horizontally toward the right wing tip, and the Z axis will extend downward, perpendicular to the X and Y axes. The origin is at the center of gravity of the airplane, which is assumed to be at the quarter mean aerodynamic chord. As the airplane pitches, it carries these axes with it.

The assumptions made to simplify the analysis are those usually made for stability calculations; namely, that (1) the airplane is a rigid body, (2) effects of angular velocity and angular acceleration upon the forces are negligible, (3) the linear and angular velocity increments are small, and (4) terms involving the products of two or more small quantities are negligible.

The longitudinal stability can be considered separately since the linear and angular velocity increments  $v$ ,  $p$ , and  $r$ , being small, do not affect  $X$ ,  $Z$ , or  $M$ , and likewise,  $u$ ,  $w$ , and  $q$  do not affect  $Y$ ,  $L$ , or  $N$ .

Using the described axes and the stated assumptions the equations of motion for the longitudinal group may be written as

$$m \frac{du}{dt} = \frac{\partial X}{\partial u} u + \frac{\partial X}{\partial w} w + \frac{\partial X}{\partial \theta} \theta$$

$$m \left( \frac{dw}{dt} - U q \right) = \frac{\partial Z}{\partial u} u + \frac{\partial Z}{\partial w} w + \frac{\partial Z}{\partial \theta} \theta$$

$$mK_y^2 \frac{dq}{dt} = \frac{\partial M}{\partial u} u + \frac{\partial M}{\partial w} w + \frac{\partial M}{\partial q} q$$

Dividing the first two equations by  $m$ , the mass, and the third by  $mK_y^2$ , the moment of inertia about the  $Y$  axis, and letting

$$\frac{\partial X}{\partial u} = X_u, \quad \frac{\partial M}{\partial u} = M_u$$

and also substituting  $\frac{d\theta}{dt}$  for  $q$ , results in the equations

$$\frac{du}{dt} - X_u u - X_w w - X_\theta \theta = 0$$

$$\frac{dw}{dt} - Z_u u - Z_w w - U \frac{d\theta}{dt} - Z_\theta \theta = 0$$

$$\frac{d^2\theta}{dt^2} - M_u u - M_w w - M_\theta \frac{d\theta}{dt} = 0$$

which contain the unknowns  $u$ ,  $w$ , and  $\theta$ . The equations are simultaneous linear differential equations and can be reduced to three homogeneous algebraic equations by substituting the differential operator  $D = \frac{d}{dt}$ . The equations become

$$\begin{aligned} (D - X_u) u - X_w w - X_\theta \theta &= 0 \\ -Z_u u + (D - Z_w) w - (UD + Z_\theta) \theta &= 0 \\ -M_u u - M_w w + (D^2 - DM_\theta) \theta &= 0 \end{aligned}$$

The condition that there shall be a solution other than the useless one  $u = w = \theta = 0$ , is that the determinant of the coefficients be equal to zero.

The determinant is

$$\begin{vmatrix} (D - X_u) & -X_w & -X_\theta \\ -Z_u & (D - Z_w) & -(UD + Z_\theta) \\ -M_u & -M_w & (D^2 - DM_\theta) \end{vmatrix} = 0$$

Expanded, the result is a biquadratic of the form

$$aD^2 + bD + cD^2 + dD + e = 0$$



The determinant, however, is in the dimensional form. Reference 8 presents a method of reducing the terms of the determinant to non-dimensional form by the use of the time factor, tau, where

$$\tau = \frac{w/s_p}{\frac{\rho}{2} g U} \quad \text{sec.} \quad ,$$

and the characteristic longitudinal length,  $l$ , of the airplane which, for conventional airplanes, is the distance from the center of gravity to the center of pressure of the horizontal tail. For the flying wing, the longitudinal distance from the center of gravity to the quarter-chord point of the mean aerodynamic chord of the tips was used as the characteristic length of the airplane.

It should be noted that the term " $S_p$ " in  $\tau$ , the time factor, is the area of the panel only, since the panel area has been used throughout as the lifting area, and the tips considered as tail area.

Using the time factor,  $\tau$ , and the length factor,  $l$ , to reduce the determinant above to non-dimensional form gives the following determinant:

$$\begin{vmatrix} (d - x_u) & -x_w & C_{L\mu} \cos \theta_0 \\ -z_u & d - z_w & C_{L\mu} \sin \theta_0 - d\mu \\ -m_u & -m_w & d^2 - dm_q \end{vmatrix} = 0$$

where  $\theta_0$  is the angle between the flight path and the horizontal

(negative in gliding flight). The term  $\mu$  is equal to  $\frac{w/s}{\frac{\rho}{2} g l}$  and is

the only factor in the determinant in which the size of the airplane appears.

It is easily shown (see Reference 8) that the non-dimensional derivatives can be written in the following form

$$\begin{aligned}x_u &= -2 C_D \\z_u &= -2 C_L \\m_u &= 0 \text{ for gliding flight} \\x_w &= C_L - \frac{dC_D}{d\alpha} \\z_w &= -\left(\frac{dC_L}{d\alpha} + C_D\right) \\m_w &= \frac{1}{b} \frac{dC_m}{d\alpha}, \text{ where } b = \frac{K}{l^2} y^2\end{aligned}$$

The rotational damping derivative  $m_q$  is to be scaled up for the full-size airplane. The explanation of this procedure will be presented later.

The numerical values of these characteristics are given in Table II.

The expansion of the determinant results in a quartic equation of the form

$$A s^4 + B s^3 + C s^2 + D s + E = 0$$

where

$$\begin{aligned}A &= 1 \\B &= -(x_u + z_w + m_q) \\C &= m_q (x_u + z_w) - (x_w z_u - x_u z_w) - \mu m \\D &= m_q (x_w z_u - x_u z_w) + \mu m_u (C_L \cos \theta_0 - x_w) + \mu m_w (C_L \sin \theta_0 + x_u) \\E &= \mu C_L m_w (\cos \theta_0 z_w - x_u \sin \theta_0) - \mu C_L m_u (\cos \theta_0 z_w - x_w \sin \theta_0)\end{aligned}$$

For complete stability, each root of the quartic must be "pseudo-negative"; that is, the value must be negative if the root is real, or the real part must be negative if the root is complex.

The condition that the roots be pseudo-negative is obtained when each of the coefficients A, B, C, D, and E is positive and when Routh's Discriminant

$$R = BCD - B^2E - AD^2$$

is also positive.

All that remains to be done before the coefficients can be evaluated is to scale the value of the damping coefficient "c" for the model to the non-dimensional derivative "m" for the full-size airplane. As is shown in Reference 9, the relation between the model coefficient and that of the full-size airplane is

$$\left(\frac{\partial M}{\partial q}\right)_{\text{full size}} = \left(\frac{\partial M}{\partial q}\right)_{\text{model}} \times (\text{scale ratio})^4 \times \frac{V_{\text{full size}}}{V_{\text{model}}}$$

The term  $\left(\frac{\partial M}{\partial q}\right)_{\text{model}}$  is the damping coefficient c, the scale ratio is the ratio of airplane span to model span (always greater than one), while the velocity ratio is that of the full-size airplane for the tested angle of attack, to that at which the model was tested. The latter can be computed from the records of q, temperature, and pressure taken at the time of the testing. The velocity of the full-size airplane for the angle of attack tested is calculated from the angle of glide, the tangent of the angle being  $\frac{C_L}{C_D}$ . From these values,  $\left(\frac{\partial M}{\partial q}\right)_{\text{full size}}$  can be found. To transform the dimensional derivative  $\frac{\partial M}{\partial q}$  to the non-dimensional form,  $m_q$ , it is divided by the moment of inertia of

the full-size airplane and then multiplied by the time factor,  $\tau$ .  
The values of these factors are given in Table II.

The coefficients of the quartic equation

$$Ad^4 + Bd^3 + Cd^2 + Dd + E = 0$$

can now be calculated and Routh's Discriminant evaluated.

It is shown in Reference 1 that if the coefficients are of such a ratio that

$$C > B$$

$$C^2 > 20E$$

and

$$CB > 20D$$

then the quartic can be factored with sufficient accuracy into

$$(d^2 + Bd + C) \left[ d^2 + \left( \frac{D}{C} - \frac{BE}{C^2} \right) d + \frac{E}{C} \right] = 0$$

The oscillation indicated by the first term of the factorization is of short period and so heavily damped that it is of no importance unless the analysis is concerned with the motion during the first three seconds after the initial disturbance. The oscillation indicated by the second part of the factorization is of long period and is slightly damped. It is the oscillation known as the "Phugoid". This is the motion with which the present investigation was concerned.

It is shown in Reference 1 that the damping factor of the phugoid is closely approximated by the relation

$$DF = \frac{1}{2\tau} \left( -\frac{D}{C} - \frac{BE}{C^2} \right)$$

while the frequency of the oscillation is

$$\omega = \frac{1}{J} \sqrt{\frac{E}{C} - \frac{1}{4} \left( \frac{D}{C} - \frac{BE}{C^2} \right)}$$

The period,  $T$ , is then

$$T = \frac{2\pi}{\omega}$$

the time to damp to one-half is

$$t_{\frac{1}{2}} = \frac{\log_e 2}{D F}$$

and the number of oscillations occurring before the amplitude is damped to one-half amplitude is

$$n_{\frac{1}{2}} = \frac{t_{\frac{1}{2}}}{T}$$

These criteria of the dynamic longitudinal stability of the full-size flying wing were calculated for four angles of attack, ranging from that for extreme high speed to that for near stalling, and are plotted in Figure 18. Figures 15, 16, and 17 show the variation of the non-dimensional resistance derivatives with angle of attack.

## DISCUSSION

The curve of  $C_L$  versus angle of attack (Figure 8) shows that the stall is not abrupt, especially for angles of tip depression up to twenty-five degrees. This delayed stall effect is probably due to the fact that the tips, being at a lesser angle of attack than the panel, still have some lift when the panel is at the point of stall. The point at which the depressed tips begin to exert positive lift is indicated by the point on the lift curve at which the slope increases. This characteristic of delayed stall is favorable to stability in the stalled attitude, and was predicted by stable flights from the glider with the center of gravity located rather far back and the path of descent unmistakably indicating a stalled condition. It was in these glides, however, that the model was most apt to develop a phugoid oscillation, and a dynamic test at a stalled attitude would be necessary to determine the exact measure of stability.

Figure 11, the curve  $C_L$  versus  $C_D$ , shows a rather high minimum  $C_D$  considering that the parasite drag (defined as "all drag less wing drag", not "all drag less induced drag" as is commonly done) is zero, and that the coefficients are based on panel area only. The low value of  $C_{Lmax}$  may also be attributed partially to basing the coefficients on the panel area. A favorably slow increase of  $C_D$  with  $C_L$  is indicated, especially up to lift coefficients usually attained in non-acrobatic flight.

The curve of moment coefficient versus angle of attack (Figure 10) shows marked static stability up to a high angle, depending on the angle

of tip depression. The greater the angle of depression, the longer the tip is acting at a negative angle and exerting a stabilizing down load behind the center of gravity.

The coefficient  $C_m$  is that at the quarter-chord point of the mean aerodynamic chord of the panel, at which point the center of gravity was assumed to be located. It is seen from Figure 10 that the largest angle of attack that can be maintained for this center of gravity location is about six degrees, and then only with a tip depression of forty degrees. When this investigation was begun, it was believed that the wing tips could be made to act as elevators and ailerons, and that no other control surfaces would be required. It appears, however, that the tips are more comparable to the stabilizer on a conventional airplane. As was mentioned in the section discussing the testing of the gliders, a certain amount of control was attainable by adjusting the tip depression angle. However, since the  $C_m$  versus  $\alpha$  curve indicates that an angle of attack of only six degrees is attainable from tip angle variation, it is evident that extra control surfaces are necessary for a wing of these proportions. The best procedure seems to be to use the tips to trim the airplane for slight center of gravity movements and speed variations, and to incorporate control surfaces on the trailing edges of the tips or panel to give the required amount of longitudinal control. Further investigation would be necessary to determine the best position and size of these controls.

The curve of lift over drag ratio versus angle of attack (Figure 12) show that the highest value of  $L/D_{max}$  is obtained with a tip depression of from ten to twenty-five degrees. This angle of tip depression is un-

doubtedly a function of the tip size, and the angle between bend line and thrust line. It may also be noted that the greater the angle of tip depression, the larger the angle of attack at which the maximum value of lift over drag ratio occurs. This fact can be explained by considering the relative angles of attack of tips and panel. When depressed, the tips are operating at smaller angles of attack than the panel. Thus, the  $L/D_{\max}$  increment due to the depressed tips occurs at a larger "airplane" angle of attack than that due to the panel and so tends to shift the point of  $L/D_{\max}$  for the whole airplane to a larger angle.

The maximum value of lift over drag ratio obtained is shown to be only 11.2. However, the Reynolds numbers at which the tests were made are low, being in the neighborhood of 180,000. Force tests made at low Reynolds numbers must be expected to yield slightly low values for lift and somewhat high values for drag.

These facts indicate that the  $L/D_{\max}$  values obtained for the flying wing model are undoubtedly lower than can be expected for the full-size airplane. An approximation of the correct magnitude of  $L/D_{\max}$  can be made by increasing the value read from the curve (Figure 11) by 22 per cent. This percentage was arrived at by a comparison of  $L/D$  values for a Clark-Y airfoil obtained in the tunnel in which the flying wing model was tested, with the  $L/D$  values for a Clark-Y airfoil as given in various text books. The comparison indicates that the values obtained in this tunnel with open-jet are approximately 22 per cent low. This indication is further substantiated by the fact that  $L/D_{\max}$  for a Lockheed Vega model tested in the tunnel was ten, while twelve is about the



correct value for this airplane.

In view of the above statements, it would seem that a value of  $L/D$  max of fourteen could be expected for the full-size flying wing. This value is comparable to that of clean, conventional type airplanes.

Figures 15, 16, and 17 show the variation of the non-dimensional resistance derivatives with angle of attack. Table II gives the derivatives expressed in the aerodynamic characteristics of the airplane. The variation of the derivatives is similar to that for any stable airplane, with the exceptions of the change in slope of the  $m_w$  curve and the increase, in the negative direction, of  $m_q$  with  $\alpha$ . Considering the aerodynamic expression for  $m_w$ ; i. e.,  $m_w = \frac{L^2}{K_y} \frac{dC_m}{d\alpha}$ , it is seen that the reversal of the curve is due to the decrease in the negative slope of the static pitching moment coefficient curve (Figure 10) at the higher angle of attack. The fact that the damping coefficient in pitch,  $m_q$ , increases with angle of attack seems unusual, and has only the oscillation test data to substantiate it. It should be stated here that the oscillation tests at the largest angle of attack, eleven degrees, were the least consistent of all. There being some pulsation or irregularity of flow in the wind stream, the oscillations of the model were not perfectly regular, and an average of a number of runs for time to damp was taken. The regularity of oscillation was most disturbed at the eleven degree angle of attack, although the maximum per cent of difference between the average and any given run of time to damp was no greater for the eleven degree tests than for the tests at the smaller angles of attack.

The results of the stability calculations are shown in Figure 18.

The usual criteria of stability; namely, period of oscillation , and time to damp to one-half amplitude, are plotted against angle of attack. In the same figure, frequency and damping factor are also shown against angle of attack. Since the period of the oscillation is  $2\pi$  divided by the frequency, and the time to damp to one half is the log 2 divided by the damping factor, a discussion of period and time to damp will also apply to the other two factors.

The period of the oscillation resulting from an initial disturbance is seen from the curve to have a minimum value of about twenty-four seconds at an angle of attack of 8.5 degrees. This oscillation is certainly slow enough to be unobjectionable to passengers and pilot, except that were it to continue, it might cause air sickness. The plot of time to damp to one-half amplitude, however, shows that at this angle of attack the oscillation will be reduced to one-half amplitude in twenty-three seconds, which indicates that the oscillation would die out very rapidly even if uncorrected by the pilot.

At the larger angle of attack of eleven degrees, the period has the slightly greater value of twenty-seven seconds. This increase from a minimum of twenty-three seconds at 8.5 degrees seems to indicate that the oscillations do not become increasingly rapid at near stalling, i.e. near landing, attitude, and is a very desirable characteristic. While the time to damp to one-half amplitude has also increased somewhat, being about twenty-eight seconds at this attitude, it has relatively little importance here since when landing, the pilot will be especially alert and by use of the controls would at once correct any disturbance.

The previously described lift curves (Figure 8) show that the landing attitude of the airplane will be about thirteen and one-half degrees. No oscillation tests were made at this angle of attack. However, from the shapes of the period and time to damp to one-half amplitude curves at eleven degrees, it is believed that there will be a good degree of stability even at the landing attitude, as compared with the decreasing stability of conventional airplanes as the stall is approached.

The curve of time to damp to one-half amplitude shows a maximum value for the lower angle of attack; i.e., higher speed, range at five degrees. Even at this point the oscillations will be reduced to one-half amplitude in twenty-six seconds, if allowed to persist, and at lower angles of attack, the damping is increasingly heavy.

The period of the oscillation becomes increasingly great as the angle of attack is decreased below eight degrees. Under normal steady flight conditions, the period will be on the order of thirty to sixty seconds which is so slow an oscillation as to be unconsciously corrected by the pilot in straight and level flight.

## CONCLUSIONS

The following conclusions can be drawn in regard to the tested flying wing design:

1. The phugoid oscillation at the lowest angle of attack is very stable, being of long period and heavily damped.
2. There is a good degree of stability even at angles of attack approaching the stalling angle, although the period and damping are both less than at the lower angles. Indications are that the oscillation will also be stable for the stalled attitude.
3. The maximum value of lift over drag ratio will be approximately that of clean, conventional airplanes.
4. From the standpoint of unrestricted field of gunfire, the flying wing design should be well suited to military use.
5. The simplicity of construction and consequent reduced cost of manufacture, along with the large amount of available space within the thick wing makes the design suitable for large cargo carrying airplanes.

## BIBLIOGRAPHY

1. Bairstow, Leonard, Applied Aerodynamics. New York: Longman, Green and Co., Second Edition, 1939, pp.753-764.
2. Hunsaker, H., Dynamical Stability, Smithsonian Miscellaneous Collections, 1917, Vol. 62, No. 5.
3. Knight, Montgomery, "Theory of Vibrations". Unpublished lecture notes, Daniel Guggenheim School of Aeronautics, Georgia School of Technology, 1941-42.
4. Mahoff, G. A., L. B. Rumph, and W. R. Weems, "Calibration of Small Wind Tunnel at the Georgia School of Technology". Unpublished student technical report, Daniel Guggenheim School of Aeronautics, Georgia School of Technology, Report No. 4, 1932-33, 15 pp.
5. Miller, M. P., An Accurate Method of Measuring the Moments of Inertia of Airplanes, U.S. National Advisory Committee for Aeronautics, Technical Report No. 351, 1930.
6. Poulsen, C. M., "The Fighting Pterodactyl", Flight, XXVI (September 6, 1934), pp.914-916.
7. Van Schlietett, G., Experimental Verification of Theodorsen's Theoretical Jet-Boundary Correction Factors, U.S. National Advisory Committee for Aeronautics, Technical Report No. 506, 1934.
8. Weems, W. R., "Dynamic Stability". Unpublished lecture notes, Daniel Guggenheim School of Aeronautics, Georgia School of Technology, 1939.
9. Wilson, E. B., Aeronautics. New York: John Wiley and Sons, Inc., 1920, p.103.

**APPENDIX**

## APPENDIX

I CALCULATION OF  $I_{YY}$  OF THE MODEL

The model was suspended in the cradle (see Figure 13) with the lateral axis parallel to the axis of suspension, and then swung through a small arc.

Reference (6) gives the following equation for the moment of inertia:

$$I_{YY} = \frac{W T^2 L}{4} - \frac{W L^2}{g}$$

where

$I_{YY}$  = moment of inertia about the axis  
through the c.g. of the model

W = weight of the model  
= .644 lbs.

T = period of oscillation  
= .675 sec.

L = distance from model c.g. to axis  
of oscillation  
= 4.36 inches

substituting,

$$I_{YY} = .000063 \text{ lb.ft.sec.}^2 \text{ (or slug-ft.}^2\text{)}$$

The equation in Reference (5) contains terms which take into account the weight, c.g. location, and period of the cradle. In the present case the cradle was so light, and its airdamping so small as compared to the model, that its effect was considered negligible.

## II CALCULATION OF $I_{YY}$ FOR THE FULL-SIZE AIRPLANE

The full-size airplane has the following specifications:

span	= 40 ft.
center section chord	= 9.66 ft.
tip chord	= 1.64 ft.
airfoil section	= 0021

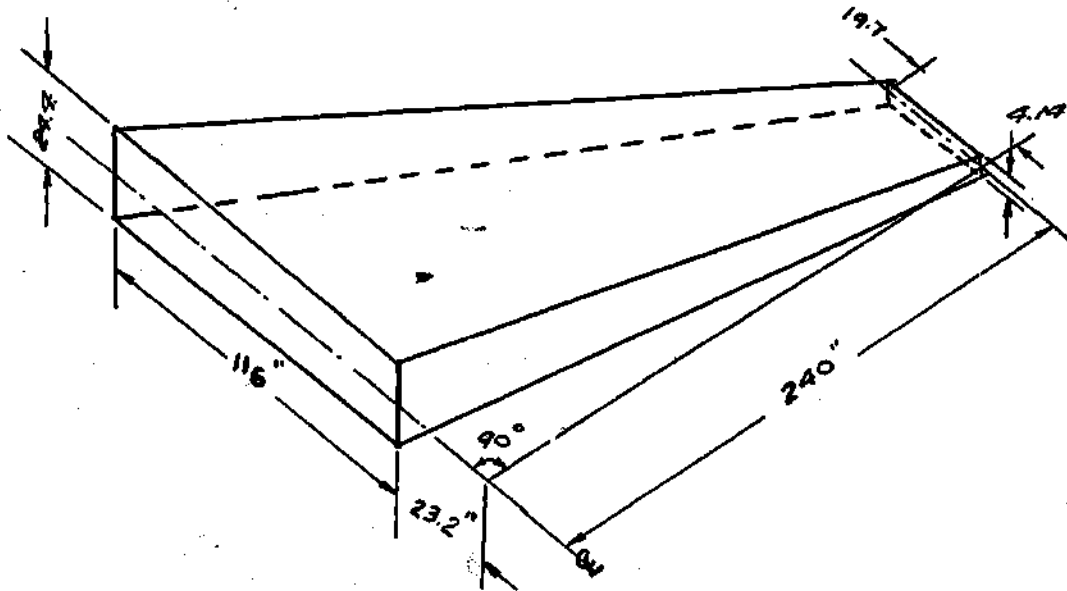
The weights are

landing gear	150 lbs.
engines ( 2 at 125 H.P.)	500 "
gas and oil (35 gal.)	240 "
pilot and equipment	250 "
structure	<u>1520</u> "
Total	= 2660 lbs.

The geometric shape was scaled directly from the wind tunnel model using the scale ratio of 23.2 : 1.

The structural weight of the wing was considered, for moment of inertia calculations, to be proportional to the volume. The section of the wing was assumed to be rectangular. With these assumptions the weight per unit volume was calculated as follows:





Semi-wing

$$\text{Vol.} = \frac{1}{3} h (B + b + \sqrt{Bb})$$

where

$h$  = normal distance from C to tip  
= 240 in.

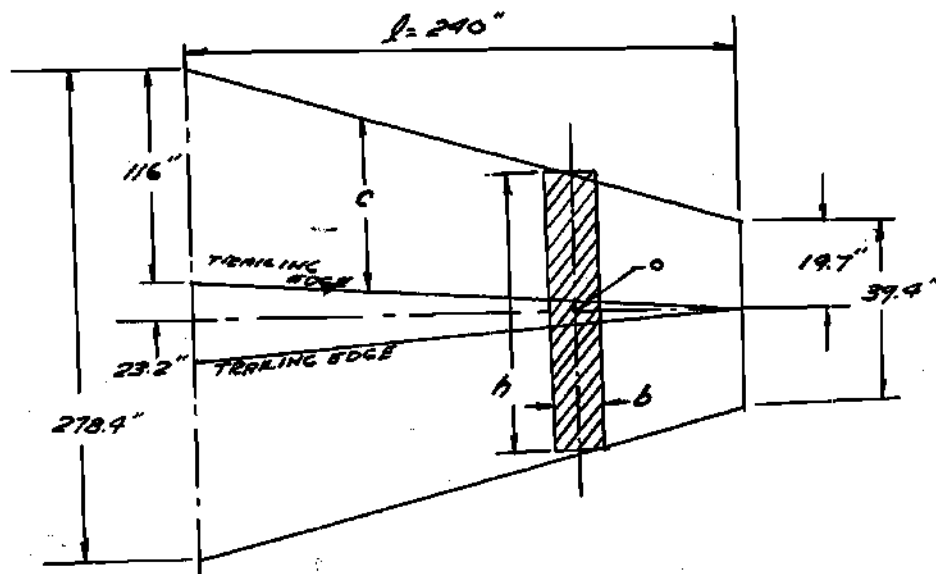
$B$  = area of cross section at C  
= 2830 in.<sup>2</sup>

$b$  = area of cross section at tip  
= 81.5 in.<sup>2</sup>

Vol. = 271,320 cu.in. for the semi-wing

$w$  = weight/cu.in. = structural wt./ total cu.in.  
= .0028 lbs./in.

To facilitate the calculation of  $I_{yy}$  for the wing structure, the wing was assumed to be cut in two, the trailing edges of the tips placed together, and the center sections lined up as shown in the figure on the following page. Then, assuming the space between the trailing edges to have the same solid density as the wing, the  $I_0$  of the resulting body was as shown.



The polar moment,  $J_p$ , of the rectangular cross-section is

$$J_p = \frac{b h^3 + h b^3}{12}$$

Then for the whole body the mass moment of inertia,  $I_o$ , is

$$I_o = \frac{w}{12g} \int_0^l \left( \frac{b h^3 + h b^3}{12} \right) dx$$

where  $dx$  is taken from the  $\frac{1}{2}$  to the tip.

The thickness,  $b$ , of the wing was assumed to be 18 per cent of the chord,  $c$ , or, within close enough limits, 9 per cent of  $h$ . The true airfoil section has a maximum thickness of 21 per cent.

It can be seen from the figure that  $h$  can be expressed as

$$h = 278.4 - \frac{239}{240} x$$

Substituting this expression in the equation for  $I_o$ , and integrating from 0 to 1, 240 gives

$$I_o = 1540 \text{ lb.ft.sec.}^2 \text{ (slug-ft.}^2\text{)}$$

The moment of inertia of the wedge portion alone is found in the same manner. The relations for the thickness and "chord" of the wedge are

$$b_w = 25.06 - \frac{21.51}{240} x$$

and

$$h_w = 26.4 - \frac{26.4}{40} x$$

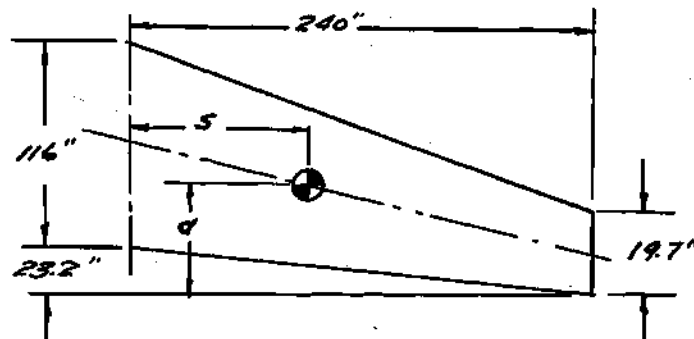
They are substituted in the equation

$$I_{ow} = \frac{w}{12g} \int_0^{240} \left( \frac{b_w h_w^3}{12} + \frac{h_w b_w^3}{12} \right) dx$$

which evaluated gives

$$I_{ow} = 2 \text{ slug-ft.}^2$$

Subtracting this from the moment of inertia of the whole body gives 1538 slug-ft.<sup>2</sup> as the moment of inertia of the "box wing" structure about a lateral axis through the trailing edges of the wing tips.



The center of gravity of the "box wing" is on the line joining the midpoints of the center section and tip section. Its distance,  $S$ , from, and normal to, the center line is

$$S = \frac{h (A + 2\sqrt{AB} + 3B)}{4 (A + \sqrt{AB} + B)}$$

where

$h$  = semi-span = 240 in.

$A$  = area of the center section = 2830 sq.in.

$B$  = area of the tip section = 81.5 sq.in.

Substituting these values gives

$$S = 71.4 \text{ in.}$$

By proportion, the distance  $d$ , from the c.g. to the axis through the tip trailing edges, is

$$d = 59.95 \text{ in.}$$

The moment of inertia,  $I_{YY}$ , of the "box wing" about its lateral axis through the c.g. is found by

$$I = I_{YY} + m d^2$$

$$I_{YY} = 360 \text{ slug-ft.}^2$$

This moment of inertia of the "box wing" about its c.g. axis was assumed to be the moment of inertia of the true wing about its lateral axis through the quarter-chord point of the mean aerodynamic chord of the panel. From a consideration of the shape and probable structure of the true wing, it is believed that the c.g. of the wing structure will be close to the quarter mean aerodynamic chord, making

the above assumption reasonable.

The positions of the remaining items were estimated by use of a drawing of the model and their moments of inertia about the y axis arrived at as follows:

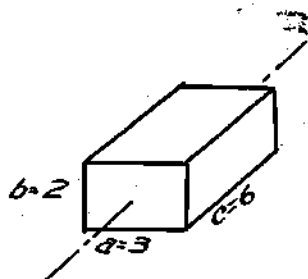
### Motors

location - 1 in. (23.2) aft of y axis

(23.2 = scale ratio of drawing)

size - 3 by 2 by 6 ft.

weight - 500 lbs.



$$I_o = \frac{W}{12g} (a^2 + b^2)$$

$$= \text{approx. } 20 \text{ slug-ft.}^2$$

$$I_{yy} = I_o + M d^2$$

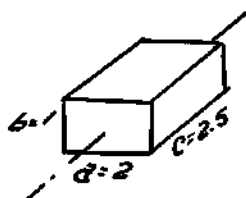
$$= \text{approx. } 90 \text{ slug-ft.}^2$$

### Fuel and tanks

location - on y axis

size - 1 by 2 by 2.5 ft.

weight - 240 lbs.



$$I_{yy} = \frac{W}{12g} (a^2 + b^2)$$

$$= \text{approx. } 5 \text{ slug-ft.}^2$$

Landing gear

location - 1.5 in. (23.2) back of yy axis

weight - 150 lbs.

$$I_o \text{ assumed} = 0$$

$$I_{yy} = M d^2$$

$$= \text{approx. } 50 \text{ slug-ft.}^2$$

Pilot and equipment

location - 3/4 in. (23.2) ahead of yy axis

weight - 250 lbs.

$$I_o \text{ assumed} = 0$$

$$I_{yy} = M d^2$$

$$= \text{approx. } 20 \text{ slug-ft.}^2$$

Summation of  $I_{yy}$  for entire airplane

Structure	360 slug-ft. <sup>2</sup>
Motors	90 "
Tanks and fuel	5 "
Landing gear	50 "
Pilot and equipment	<u>20</u> "
Total	525 slug-ft. <sup>2</sup>

$$\text{Then, } K_y^2 = \frac{I}{M} = 6.35 \text{ ft.}^2$$

$$\text{or } K_y = 2.5 \text{ ft.}$$

This value, which is believed to be a good approximation of

the radius of gyration of this airplane, was used in the stability calculations.

### III CALCULATION OF THE VELOCITY AND ANGLE OF DESCENT OF THE FULL SIZE AIRPLANE FOR THE TESTED ANGLES OF ATTACK.

In gliding flight

$$D = W \sin \theta = \frac{\rho}{2} S V^2 C_D$$

$$\text{and } L = W \cos \theta = \frac{\rho}{2} S V^2 C_L$$

$$\text{from which } \sin^2 \theta + \cos^2 \theta = 1 = \left( \frac{S}{W} \right)^2 V^4 (C_D + C_L)$$

For  $\alpha = 5$  degrees,

$$C_L = .227, \quad C_D = .032, \quad \frac{\rho}{2} = .00198$$

$$\text{and } \frac{S}{W} = 15.45 \quad (\text{based on panel area})$$

Substituting,

$$V = 238 \text{ ft./sec.} = 162 \text{ m.p.h.}$$

$$\sin \theta = \frac{\rho}{2} \frac{S}{W} V^2 C_D$$

$$= .1395$$

$$\theta = 8 \text{ deg. } 0 \text{ min.}$$

This is the angle of the flight path, and appears in the stability calculations as  $\theta_0$ .